Selective ablation of αv integrins in the central nervous system leads to cerebral hemorrhage, seizures, axonal degeneration and premature death

Joseph H. McCarty[1,*], Adam Lacy-Hulbert[1,2,3], Alain Charest[1], Roderick T. Bronson[3], Denise Crowley[1,*], David Housman[1], John Savill[2], Jürgen Roes[4] and Richard O. Hynes[1,*,†]

[1]Center for Cancer Research, Massachusetts Institute of Technology, 40 Ames Street, E17-227, Cambridge, MA 02139, USA
[2]Medical Research Council and University of Edinburgh Center for Inflammation Research, Teviot Place, Edinburgh EH8 9AG, UK
[3]Harvard Medical School, 220 Longwood Avenue, Boston, MA 02115, USA
[4]Windeyer Institute for Medical Sciences, University College London, 46 Cleveland Street, London W1T 4JF, UK

*Howard Hughes Medical Institute
†Author for correspondence (e-mail: rohynes@mit.edu)

Summary

Mouse embryos genetically null for all αv integrins develop intracerebral hemorrhage owing to defective interactions between blood vessels and brain parenchymal cells. Here, we have used conditional knockout technology to address whether the cerebral hemorrhage is due to primary defects in vascular or neural cell types. We show that ablating αv expression in the vascular endothelium has no detectable effect on cerebral blood vessel development, whereas deletion of αv expression in central nervous system glial cells leads to embryonic and neonatal cerebral hemorrhage. Conditional deletion of αv integrin in both central nervous system glia and neurons also leads to cerebral hemorrhage, but additionally to severe neurological defects. Approximately 30% of these mutants develop seizures and die by 4 weeks of age. The remaining mutants survive for several months, but develop axonal deterioration in the spinal cord and cerebellum, leading to ataxia and loss of hindlimb coordination. Collectively, these data provide evidence that αv integrins on embryonic central nervous system neural cells, particularly glia, are necessary for proper cerebral blood vessel development, and also reveal a novel function for αv integrins expressed on axons in the postnatal central nervous system.

Key words: Cerebral hemorrhage, Spastic paraparesis, Ataxia, Mouse

Introduction

Among the billions of neurons and glia in the vertebrate central nervous system (CNS) is an elaborate network of blood vessels. Besides carrying essential oxygen and nutrients to cells of the CNS, blood vessels also provide growth, guidance and survival cues that regulate various aspects of CNS development and maintenance (Louissaint et al., 2002; Mi et al., 2001; Palmer et al., 2000; Song et al., 2002; Zerlin and Goldman, 1997). In turn, cells of the CNS microenvironment provide factors that influence blood vessel growth and survival (Haigh et al., 2003). Thus, deciphering how blood vessels communicate with neurons and glia is important for understanding the proper development of both the vascular and central nervous systems.

αv integrins are necessary for proper interactions between embryonic cerebral blood vessels and brain parenchymal cells (McCarty et al., 2002). Mouse embryos containing a null mutation in the αv gene, and thus lacking all five αv integrin family members; αvβ1, αvβ3, αvβ5, αvβ6 and αvβ8, exhibit normal vascular morphogenesis except in the brain. These mutants develop intracerebral hemorrhage and die shortly after birth. By contrast, deletion of both β3 and β5 integrin subunits has no effect on cerebral vascular development (McCarty et al., 2002); however, deletion of the β8 integrin gene leads to a cerebral hemorrhage phenotype similar to that seen in the αv-null mice (Zhu et al., 2002). Thus, loss of one specific integrin, αvβ8, can account for the selective cerebral blood vessel defects observed in the αv-nulls. αvβ8 is a receptor for multiple extracellular matrix (ECM) proteins (Milner et al., 1999; Mu et al., 2002; Nishimura et al., 1994; Venstrom and Reichardt, 1995), and is reportedly expressed on embryonic and postnatal glial cells and neurons in the CNS (Nishimura et al., 1998). The molecular mechanisms underlying how αvβ8 integrin functions to regulate cerebral blood vessel integrity remain to be determined, although normal endothelial cell branching and sprouting, as well as normal pericyte recruitment and apposition to the vasculature, all occur in the brains of αv-null embryos (Bader et al., 1998; McCarty et al., 2002).

To circumvent the early neonatal lethality in the complete αv-nulls and to explore further the cellular basis for the cerebral vascular defects, we have selectively ablated αv expression in cells of the embryonic and postnatal CNS.

Ablation of αv expression on CNS radial glial cells and astrocytes leads to embryonic and neonatal cerebral hemorrhage. Deletion of αv expression on both CNS neurons and glia also leads to cerebral hemorrhage, as well as additional neurological abnormalities, including seizures, ataxia and loss of hindlimb coordination. This study proves that the αv integrin subunit expressed on neural cells, particularly glia, is necessary for proper regulation of embryonic cerebral blood vessel development. Additionally, we reveal a novel function for αv integrins on postnatal CNS axons.

Materials and methods

Mouse genotyping

All progeny were confirmed by standard PCR-based genotyping of DNA isolated from tail snips or yolk sacs. Embryo staging and analysis was performed by timed matings, with noon on the plug date defined as E0.5. The following primer sequences were used for PCR genotyping: CRE, 5′-ACCAGCCAGCTATCAACTC-3′ and 5′-TAT-ACGCGTGCTAGCGAAGATCTCCATCTTCCAGCAG-3′ (the CRE primers yield a single PCR product of ~200 bp); αv-flox, 5′-TTC-AGGACGGCACAAAGACCGTTG-3′ and 5′-CACAAATCAAGG-ATGACCAAACTGAG-3′ (PCR-mediated amplification of the αv-flox allele generates a product of 350 base pairs; the αv$^{+/+}$ or αv$^{-/-}$ alleles yield a PCR product of 250 bp); and NEO, 5′-AAGAT-GGATTGCACGCAGGTTCTC-3′ and 5′-CCTGATGCTCTTCGTC-CAGATCAT-3′ (the NEO PCR product is approximately 1000 bp).

Mouse strains

Nestin-Cre mice have been described elsewhere (Tronche et al., 1999) and were purchased from Jackson Laboratories. The Tie2-Cre mice have been previously described (Kisanuki et al., 2001). The hGFAP-Cre transgene contains a 2.2 kb fragment of the human GFAP gene driving expression of Cre cDNA. Results presented here were generated using one transgenic line containing 75-100 transgene copies.

Antibodies

The following antibodies were used for immunohistochemistry: anti-Nestin and anti-RC2 (Developmental Studies Hybridoma Bank); anti-BLBP (Nathaniel Heintz, Rockefeller University); anti-GFAP (DAKO); mouse anti-β-tubulin III (Sigma); mouse anti-Cre mAb (BabCo); mouse anti-PECAM (Pharmingen); and mouse anti-Smooth Muscle α-Actin (Sigma). The anti-myelin/oligodendrocyte specific protein, anti-neurofilament, anti-NeuN and anti-GFAP mAbs antibodies were purchased from Chemicon. Secondary antibodies used for immunofluorescence were Alexa-conjugated goat anti-rabbit, goat anti-mouse and goat anti-rat (Molecular Probes).

The anti-αv antiserum (Bossy and Reichardt, 1990) was used at a 1:200 dilution. Prior to application to sections, the diluted antiserum was pre-absorbed using αv-null acetone-extracted brain protein, prepared by standard methods (Harlow and Lane, 1999). The antiserum was then applied to unfixed or Carnoy's-fixed histological sections. The anti-β8 antiserum was generated using a synthetic peptide corresponding to the C-terminal tail of the human β8 cytoplasmic region, CTRAVTYRREKPEEIKMDISKLNAHETFR-CNF. The specificity of the anti-β8 antibody was tested using COS cell lysates transiently transfected with the pcDNA3.1 plasmid (Invitrogen) containing a human β8 cDNA. The expressed β8 protein contains a C-terminal V5 epitope tag. Alternatively, cortical astrocytes cultured from αv$^{+/-}$ or αv$^{-/-}$ neonates were cell surface labeled with EZ-Link Sulfo-NHS-LC-Biotin (Pierce). Lysates were immunoprecipitated with anti-β8, resolved by SDS-PAGE and immunoblotted with Streptavidin-HRP (Vector Laboratories).

Histology and immunohistochemistry

Adult mice were anesthetized and fixed by perfusion with 4% paraformaldehyde (PFA). For frozen embedding, adult brains were removed and post-fixed for 12-16 hours. Embryonic and neonatal brains were dissected and immersed in Carnoy's fixative or 4% PFA for 4 or 16 hours, respectively. PFA-fixed tissue was cryopreserved in sucrose at 4°C and embedded in Tissue Tek OCT (Miles). Alternatively, brains were dehydrated and processed for standard paraffin embedding and basic histological analyses. Semi-thin (1 µm) plastic sections of embryonic brains were prepared according to manufacturer's instructions (Polysciences).

Astrocyte culturing

Neonatal brains (P1-3) were removed and placed in sterile, ice-cold Hank's Balanced Salt Solution (HBSS). Whole neocortices were dissected and the hippocampus and internal structures were removed to leave only the cortical sheets. The meninges were stripped away, and the cortical sheets were minced with a razorblade and digested for 30 minutes at 37°C in Dulbecco's modified essential media containing 150 units/ml collagenase (Worthington) and 40 µg/ml deoxyribonuclease (Sigma, St Louis, MO). The cortical tissue was then triturated in DMEM containing 10% calf serum (Sigma, St Louis, MO) and filtered through a 50 µm sterile mesh. The resulting single-cell suspension was plated onto T-75 tissue culture flasks that had been pre-coated with 10 µg/ml mouse laminin (Sigma, St Louis, MO). Generally, cells from two or three neonatal brains were plated per T-75 flask. After 7-10 days the astroglial cells formed a confluent monolayer, with neurons, oligodendrocytes and fibroblasts growing on top. These contaminating cells were removed by rotary shaking the flasks overnight at 250 revolutions per minute. The resulting cultures were composed of more than 95% astrocytes, as assessed by anti-GFAP immunoreactivity. Immunostaining of cells was performed using standard procedures. Briefly, astrocytes were trypsinized and re-plated onto laminin-coated coverslips for 24 hours. Cells were fixed in 4% PFA, permeabilized in 0.1% NP40/PBS, and immunostained with primary and secondary antibodies.

Cell isolation

Adult brains were dissected and digested with collagenase and deoxyribonuclease. Brains were then minced with a razorblade and triturated to generate a cellular suspension. Brain endothelial cells were isolated using magnetic beads (Dynal) that were coated with anti-PECAM and anti-Flk rat mAbs (Pharmingen, Inc.) according to manufacturer's instructions.

Mouse behavioral analyses

A Rotarod device (Ugo Basile) was used to measure motor coordination and strength. The times at which mice fell from the rod were recorded. Mice were allowed to stay on the rod for a maximum of 360 seconds (6 minutes). Six separate trials were performed over a 2-day period (three trials per day).

Results

Vascular endothelium-specific deletion of αv integrin does not lead to cerebral vascular defects

We concluded in a previous study that αv-null mice develop brain-specific hemorrhage owing to defective associations between blood vessels and surrounding neural cells (neurons and/or glia) (McCarty et al., 2002); however, the identity of the αv-expressing cell type initiating the hemorrhage remained unknown. Analysis of αv protein expression patterns in the embryonic brain parenchyma revealed no readily detectable αv protein on endothelial cells or pericytes (Fig. 1A-F), suggesting αv integrin on cerebral vascular cells did not contribute to the cerebral hemorrhage phenotype. However, it remained possible that a low level of αv protein (undetectable by standard
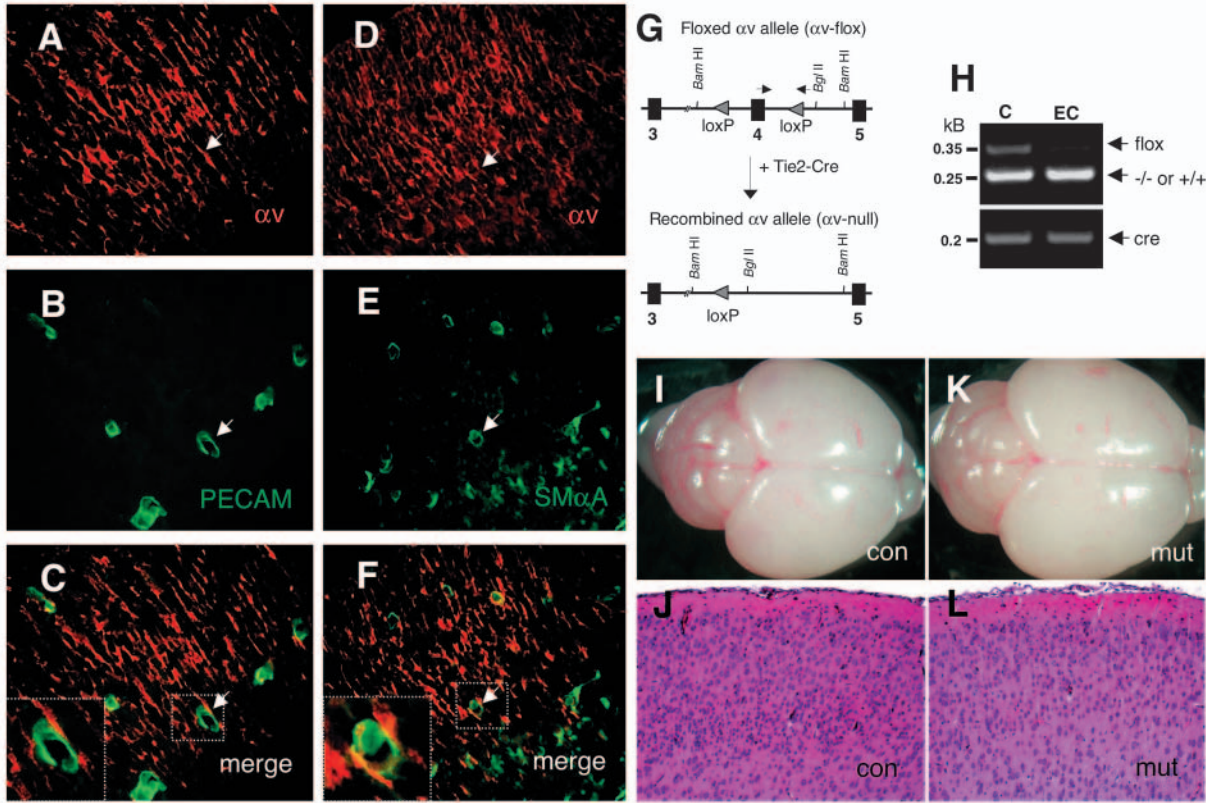
Fig. 1. Tie2-Cre conditional αv mutants do not develop cerebral vascular defects. (A-F) αv integrin is not detected on cerebral endothelial cells or pericytes. Horizontal sections through the diencephalon of an E13.5 $αv^{+/-}$ embryo labeled with pre-absorbed anti-αv antiserum (A,D), anti-PECAM (B), or anti-smooth muscle α-actin (SMαA) (E). αv protein localizes to neuroepithelial processes (A,D). (C,F) Merged images: arrows indicate close juxtaposition between αv-positive neuroepithelial processes with endothelial cells (C) and pericytes (F). Boxed areas are shown as higher magnification insets. (G) Generation of the conditional αv mutant allele in endothelial cells. Tie2-Cre-mediated recombination deletes exon four, resulting in a conditional αv-null allele (lower panel). Arrows indicate PCR primers for genotyping. (H) Cre-mediated recombination monitored by PCR using DNA isolated from PECAM/Flk1-positive brain endothelial cells (EC), or PECAM/Flk1-negative cells (C). In brain endothelial cells, there is a reduction in the intensity of the 350 bp band owing to recombination of the αv-flox allele. We confirmed deletion of exon four using a primer pair that detects the deleted αv-flox cassette (data not shown). (I-L) Brains dissected from P5 neonates. No grossly obvious cerebral vascular defects are present in control (I) or mutant (K). Hematoxylin and Eosin-stained coronal sections from control (J) and mutant (L) brains revealed no obvious microscopic neural or vascular defects.

immunofluorescence) was present, and functioned in cerebral blood vessel development. To address this possibility, we genetically ablated αv expression selectively in the vascular endothelium using the Tie2-Cre transgene (Kisanuki et al., 2001). The Tie2 promoter drives Cre expression in some hematopoietic cells, as well as the majority of vascular endothelial cells, including those comprising blood vessels of the CNS (Allende et al., 2003; Gerety and Anderson, 2002; Kisanuki et al., 2001; Liao et al., 2001).

Tie2-Cre+; $αv^{+/-}$ mice were crossed with mice containing a conditional (floxed) αv allele (A.L.-H., J.S. and J.R., unpublished). The resulting mutant progeny are hemizygous for the Tie2-Cre transgene, and carry one αv-flox and one αv-null allele. Littermate controls are hemizygous for the Tie2-Cre transgene, and carry one αv-flox and one αv wild-type allele. Recombination of the αv-flox allele by the Tie2-Cre transgene was verified using freshly isolated brain endothelial cells. Analysis of genomic DNA revealed significant reduction in the 350 bp PCR band representing the αv-flox allele (Fig. 1G,H).

Tie2-Cre+; $αv^{flox/-}$ mutants were born in expected Mendelian ratios and at birth displayed no phenotypic defects. Gross

analyses of neonatal (Fig. 1K), as well as embryonic and adult mutant brains (data not shown) revealed no obvious cerebral vascular defects. Furthermore, microscopic analysis of mutant brains showed intact cerebral blood vessels with no indication of dilation or hemorrhage (Fig. 1L). Thus, loss of αv expression in vascular endothelium does not account for the cerebral hemorrhage phenotype observed in the complete αv knockouts.

αvβ8 integrin protein is expressed on neuroepithelial processes in the embryonic brain

Previous papers using different anti-αv integrin antibodies have reported αv protein expression on embryonic neuroepithelial and radial glial cells (Anton et al., 1999; Hirsch et al., 1994). To confirm these results, we used these same anti-αv antibodies to immunostain E13.5 $αv^{+/-}$ and $αv^{-/-}$ brain sections. Surprisingly, we observed a neuroepithelial expression pattern in both $αv^{+/-}$ and $αv^{-/-}$ brain sections (data not shown). To eliminate this non-specific αv immunoreactivity, we pre-absorbed anti-αv antiserum (Bossy and Reichardt, 1990) using acetone-extracts prepared from αv-null embryos. Immunostaining $αv^{+/-}$ and $αv^{-/-}$ brain sections
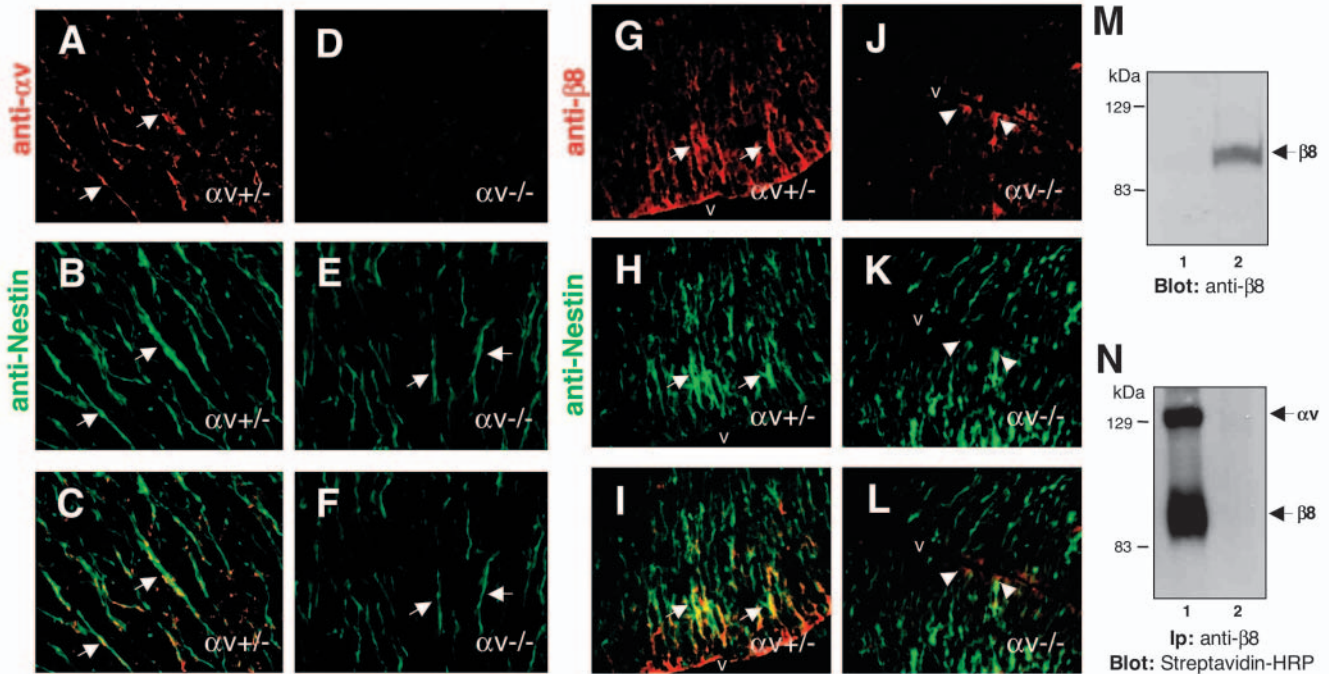
Fig. 2. αvβ8 integrin is expressed on glial cell processes in the embryonic brain. Horizontal sections through the diencephalon of E13.5 αv$^{+/-}$ (A-C) or αv$^{-/-}$ embryos (D-F) labeled with pre-absorbed specific anti-αv (A,D) and anti-nestin antibodies (B,E). (C,F) Merged images. αv integrin and nestin expression co-localize on neuroepithelial cell processes in αv$^{+/-}$ embryonic brain sections (C). No αv immunoreactivity is present on neuroepithelial cell processes from αv$^{-/-}$ brain sections (D,F). Horizontal sections through the diencephalon of E11.5 αv$^{+/-}$ (G-I) or αv$^{-/-}$ embryos (J-L) labeled with anti-β8 polyclonal antibody (G,J) and anti-nestin antibodies (H,K). (I,L) Merged images. β8-integrin and nestin expression co-localize on neuroepithelial cell processes (arrows) in αv$^{+/-}$ embryonic brain sections (I). β8 immunoreactivity is not detectable on neuroepithelial cell processes of αv$^{-/-}$ brain sections, but localizes to neuroepithelial cell bodies (arrowheads; J,L). (M,N) Specificity of the affinity-purified anti-β8 polyclonal antibody is shown using protein lysates prepared from untransfected COS cells (M, lane 1), or from COS cells transfected with cDNA encoding β8 (M, lane 2). (N) The anti-β8 antibody immunoprecipitates cell-surface-labeled αvβ8 from wild-type cultured astrocytes (lane 1), but not from αv$^{-/-}$ astrocytes (lane 2).

revealed αv-specific neuroepithelial immunoreactivity, as determined by co-localization with nestin (Fig. 2A-C). The anti-αv immunoreactivity did not colocalize with markers for newly differentiated neurons, such as β-tubulin III or MAP2 (see Fig. S1 in the supplementary material and data not shown).

Mouse embryos null for the β8 integrin subunit also develop embryonic intracerebral hemorrhage that appears identical to that in the complete αv-nulls (Zhu et al., 2002). We generated an affinity-purified polyclonal antibody directed against a peptide corresponding to the β8 cytoplasmic tail and showed that it recognized a predominant protein band of ~90 kDa from COS cell lysates transfected with a cDNA encoding the β8 protein (Fig. 2M). Analysis of primary astrocytes from wild-type neonatal mice showed that anti-β8 immunoprecipitated two cell surface proteins of ~130 kDa and ~90 kDa, both consistent with the molecular weights of αv and β8 integrins (Fig. 2N). These bands were not detected when anti-β8 was used to immunoprecipitate cell surface proteins from αv-null astrocytes (Fig. 2N). Immunostaining E11.5 αv$^{+/-}$ embryonic brain sections (Fig. 2G,I) revealed β8 protein expression on neuroepithelial cells. However, using double-label immunofluorescence analyses, no β8 protein expression was detected on endothelial cells or pericytes that comprise cerebral blood vessels (data not shown). We detected β8 protein expression in αv-null embryos; however, the spatial pattern was abnormal: β8 protein was not detectable on neuroepithelial cell processes (Fig. 2K), but was primarily localized to

neuroepithelial cell bodies (Fig. 2J,L). Thus, we concluded that, in the embryonic brain, αvβ8 integrin is expressed on glial cell processes, and that it is likely that the loss of αvβ8 expression on these cell types leads to intracerebral hemorrhage.

Neural cell deletion of αv integrin leads to cerebral hemorrhage

We attempted to ablate αv expression selectively on embryonic and postnatal glial cells using Cre under the control of the human GFAP promoter. In most mammalian species, GFAP is expressed primarily by postnatal astrocytes; however, in primates, GFAP is also expressed by embryonic radial glia and independently generated hGFAP-Cre transgenes show Cre expression in both embryonic and post-natal glial cells (Bajenaru et al., 2002; Malatesta et al., 2003; Marino et al., 2000; Zhuo et al., 2001).

We used an anti-Cre antibody to monitor Cre protein expression in our hGFAP-Cre transgenics. Nuclear Cre protein was most prominent in cells adjacent to, and occasionally within, the ventricular zone of the neocortex (Fig. 3A,B) and ganglionic eminence (data not shown) as early as E15. Based on this pattern, we analyzed whether Cre protein was present in radial glial cells. Using antibodies recognizing the brain lipid-binding protein (BLBP) and the astrocyte-specific glutamate transporter (GLAST) (Anthony et al., 2004; Malatesta et al., 2003), we showed Cre protein in many cortical

radial glial cells in E15 embryos (Fig. 3A,B). By contrast, at E15, no co-localization of Cre and β-tubulin III (a marker for neurons) was detected in the neocortex (Fig. 3C) or ganglionic eminence (data not shown). Cre protein was also expressed by many GFAP-positive Bergmann glia in the cerebellum as well as astrocytes in the neonatal cerebral cortex (Fig. 3D,E). hGFAP-Cre transgene expression in astrocytes and neurons was also observed in vivo using the Rosa26-LoxSTOPLox-*lacZ* reporter strain (Soriano, 1999) to monitor hGFAP-driven

Cre activity (data not shown). Owing to their multi-potential nature, CNS radial glial cells give rise to neurons throughout the brain (Anthony et al., 2004; Malatesta et al., 2003). Therefore, it is likely that in our hGFAP-Cre strain, some embryonic and postnatal neurons may lack αv expression. Any contributions that these neurons normally make to cerebral blood vessel function would also be defective in the hGFAP-Cre conditional αv mutants.

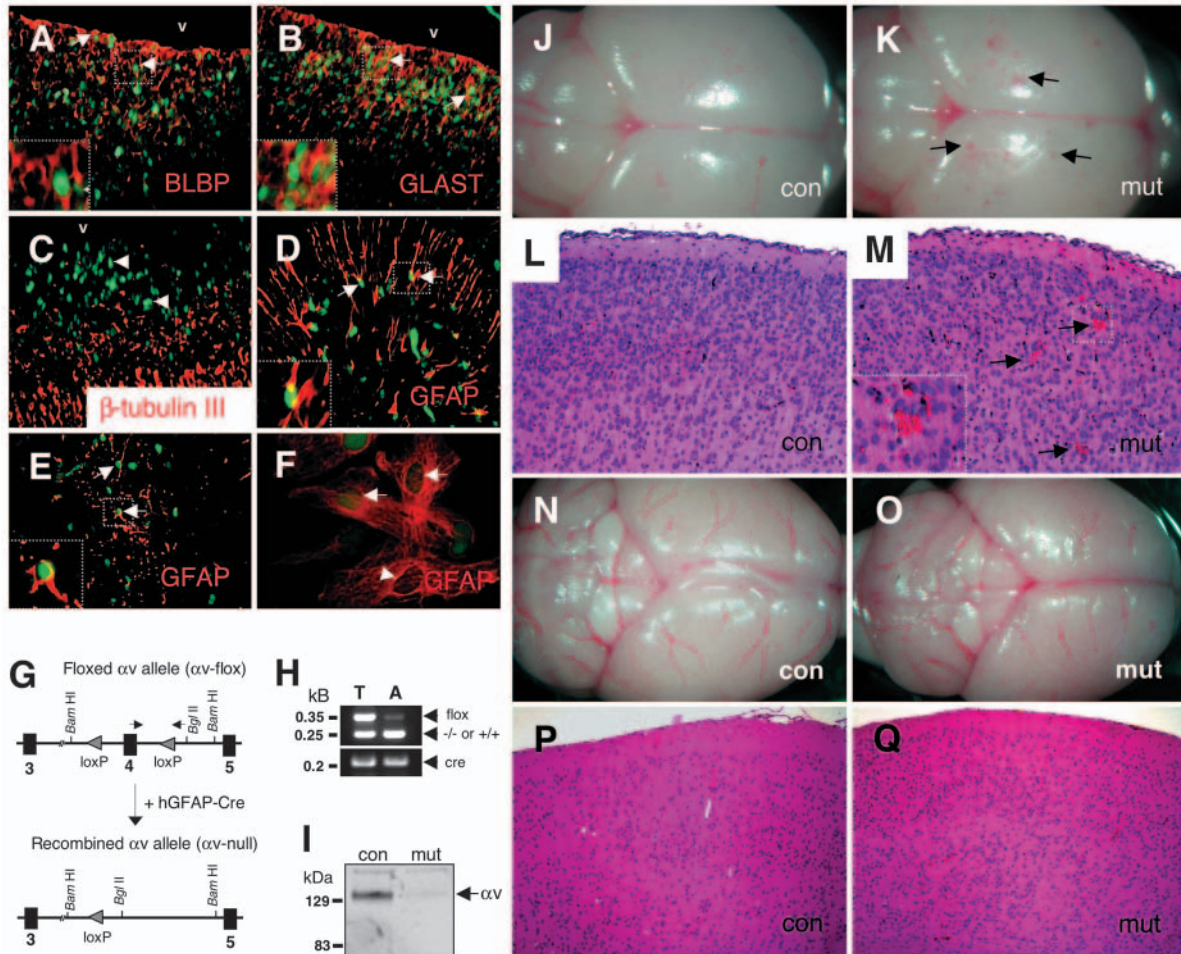Consistent with the mosaic Cre protein expression pattern in

Fig. 3. Conditional deletion of αv integrin in neural cells leads to cerebral hemorrhage. (A-F) The hGFAP-Cre transgene is expressed in central nervous system radial glial cells and post-natal astrocytes. (A,B) Sagittal sections through E15 embryonic neocortex immunostained with anti-Cre (green) and anti-brain lipid-binding protein (BLBP) (red, A) or anti-glutamate transporter (GLAST) (red, B). Expression of Cre is seen in radial glial cells within the embryonic neocortex (arrows). Regions highlighted within the dashed boxes are shown as higher magnification insets. (C) Cre is not expressed by embryonic neurons. E15 sagittal brain sections were immunostained with anti-Cre (green) and anti-β-tubulin III (red). Cre expression is absent in β-tubulin III-positive neurons (arrowheads in C). v, ventricle. (D,E) Postnatal astrocytes in the cerebellum (D) and cerebral cortex (E) express Cre. Sagittal sections from postnatal (P7) brains immunostained with anti-Cre (green) and anti-GFAP (red). There is co-localization of GFAP and Cre in cortical astrocytes in the cerebral cortex (arrows in E) as well as in Bergmann glia of the cerebellum (arrows in D). Boxed areas are shown as higher magnification insets. (F) Cultured astrocytes from hGFAP-Cre transgenic mice show mosaic Cre expression. There is co-localization of Cre and GFAP in most cells (arrows); however, some GFAP-positive cells show no detectable Cre protein expression (arrowhead). (G) Strategy for generating the conditional αv mutant allele in central nervous system neural cells, particularly glia. (H) hGFAP-Cre-mediated recombination was monitored by PCR using DNA isolated from tails (T) or from mutant cultured astrocytes (A). DNA isolated from astrocytes shows reduced intensity of the 350 bp band, owing to recombination of the αv-flox allele. We confirmed deletion of exon four using a primer pair that detects the deleted αv-flox cassette (data not shown). (I) Cortical astrocyte lysates were immunoblotted with anti-αv antibody. There is a significant reduction in αv protein expression in mutants. (J,K) Brains dissected from control (J) and mutant (K) P5 neonates. Arrows in K indicate microhemorrhage in the mutant cerebral cortex. (L,M) Coronal sections from control (L) and mutant (M) mice indicate focal regions of hemorrhage in mutant cerebral cortex (arrows in M). Boxed area shown at higher magnification (inset in M). (N-Q) Gross analysis of adult brains from control and mutant mice. Adult control (N) or mutant (O) brains do not display overt signs of cerebral microhemorrhage. Hematoxylin and Eosin stained coronal sections from adult control (P) and mutant (Q) cerebral cortex reveal normal cytoarchitecture and no microscopic hemorrhage.
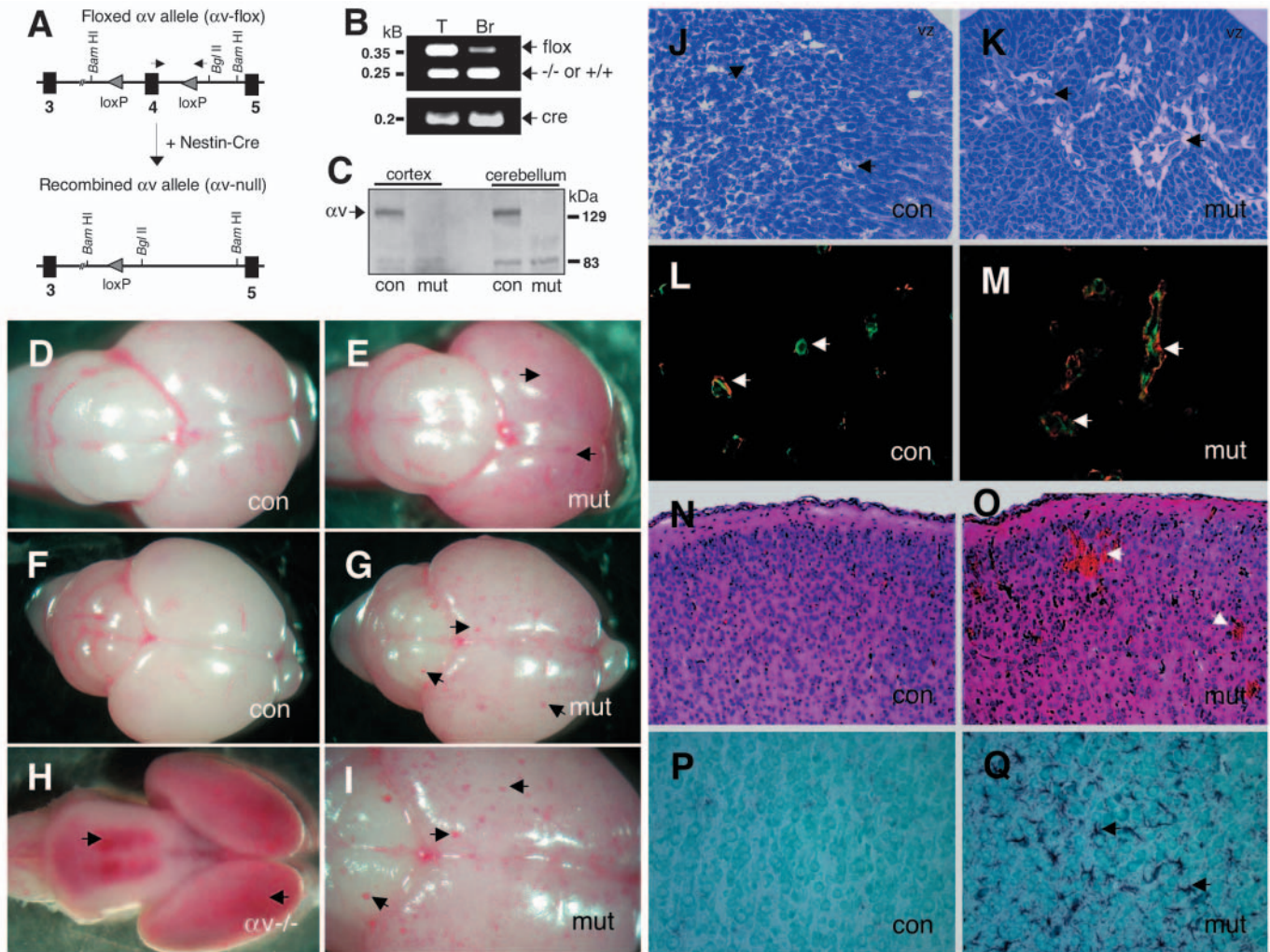
Fig. 4. Conditional deletion of αv integrin in both CNS neurons and glia leads to cerebral hemorrhage. (A) Generation of the conditional αv mutant allele in CNS glia and neurons. (B) PCR performed using DNA from mutant tail (T) or brain (Br) tissue. In a sample from the brain, the intensity of the 350 bp band is significantly reduced, owing to Cre-mediated recombination of the αv-flox allele. We confirmed deletion of exon four using a primer pair that detects the deleted αv-flox cassette (data not shown). (C) Lysates from the cerebellum and cortex were immunoblotted with anti-αv antibody. There is marked reduction in αv protein levels in the mutant brains, indicating Cre-mediated deletion of αv gene expression. (D-G,I) Control or mutant brains dissected from E17.5 embryos (D,E) and P7 neonates (F,G,I). Unlike the control brains (D,F), there are obvious regions of cerebral hemorrhage present throughout the forebrain and midbrain regions of the mutant brains (arrows in E,G,I). Significantly more severe cerebral hemorrhage is seen in the complete αv-nulls (H). (J,K) Horizontal semi-thin sections from the ganglionic eminence region of E14.5 control (J) and mutant (K) brains. Vessels in the control brain are closely juxtaposed to the surrounding parenchyma (arrows in J). There are distended and tortuous vessels that separate from the surrounding neural tissue in the αv conditional mutant brain (arrows in K). vz, ventricular zone. (L,M) Horizontal sections from the ganglionic eminence of E14.5 control (L) and mutant (M) embryonic brains stained with anti-PECAM (green) and anti-NG2 (red) antibodies to reveal endothelial cells and pericytes/vSMCs, respectively. The mutant vessels lined with vascular endothelium have a distended appearance and there is surrounding coverage by pericytes (arrows in M). (N-Q) Coronal sections through the cerebral cortex of control (N) or αv mutant (O) P7 brains stained with H&E; normal neuronal patterning is observed in both. However, focal regions of hemorrhage are associated with many blood vessels in the mutant cerebral cortex (arrows in O). Coronal sections were stained with an anti-GFAP antibody to visualize astrocytes in control (P) and mutant (Q) cerebral cortex. Elevated numbers of astrocytes are present throughout the cortex of αv mutant brain (arrows in Q).

vivo, most astrocytes cultured from hGFAP-Cre mice expressed Cre, but some had no detectable level of Cre expression (Fig. 3F). PCR analysis of DNA from cultured astrocytes revealed a significant reduction in the 350 bp band representing the αv-flox allele (Fig. 3G,H). Likewise, using extracts prepared from control and mutant astrocytes, we showed a significant reduction in αv protein expressed in cells isolated from hGFAP-Cre conditional αv mutant brains (Fig. 3I). αv expressed by contaminating cells may account for the low

residual level of αv protein, although our astrocyte cultures are generally more than 95% pure (GFAP positive). The low level of αv protein present in the mutant astrocyte cell cultures was most likely due to the mosaic expression pattern of the hGFAP-Cre transgene.

hGFAP-Cre+; αv+/– progeny were mated with mice containing a loxP-flanked (floxed) αv allele (Lacy-Hulbert et al., submitted). Thus, the resulting mutant progeny are hemizygous for the hGFAP-Cre transgene, and carry one αv-
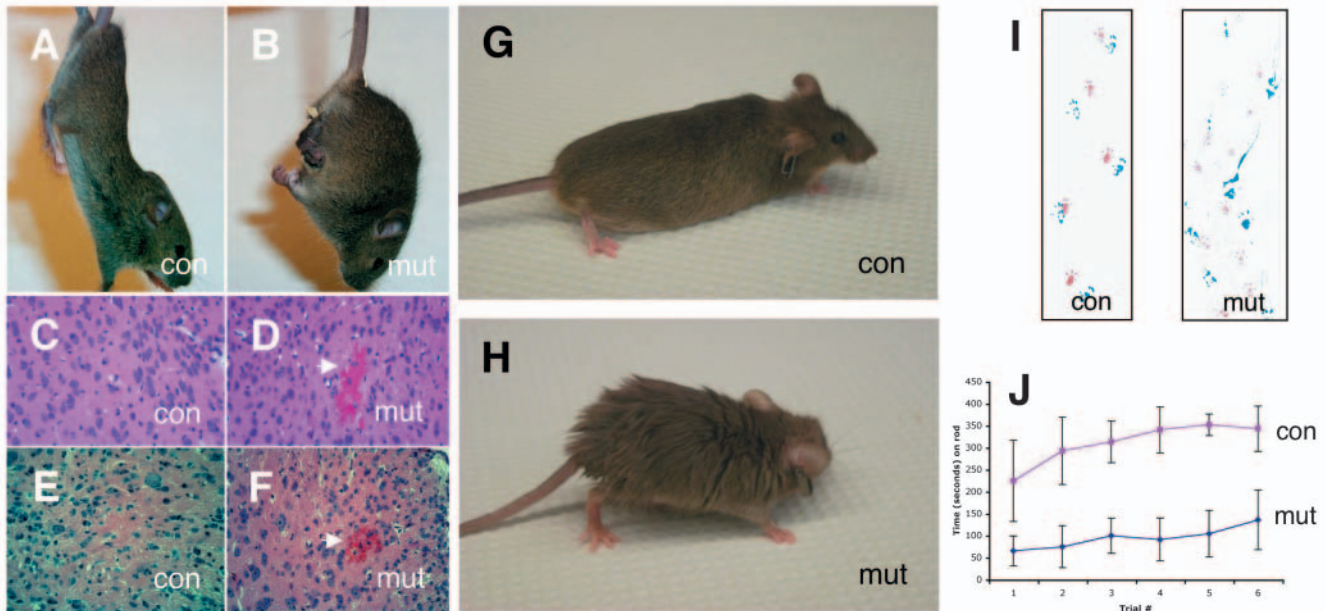
Development

Fig. 5. Nestin-Cre conditional αv mutants develop seizures and motor dysfunction, and die prematurely. (A,B) Motor dysfunction in 3-week-old Nestin-Cre conditional αv mutants. When lifted by their tails, control mice (A) extend and flail their limbs. Conditional αv mutants (B) retract their limbs and remain immobile. The conditional αv mutant in B also displayed episodic signs of seizures and associated temporary loss of consciousness (data not shown). (C,D) Hematoxylin and Eosin-stained coronal sections from cerebral cortices of three-week-old control (C) and mutant (D) brains from mice shown in A,B. Regions of cerebral microhemorrhage are present in the mutant brains (arrow in D). (E,F) Cross-sections from control (E) and mutant (F) spinal cords. Focal regions of microhemorrhage are found throughout spinal cord of conditional αv mutants (arrow in F). (G,H) Pictures of 7-month-old control (G) and mutant (H) animals. The mutant displays hind-limb spasticity and abnormal posture. (I) Footprint analysis performed using 4- to 5-month-old control (left panel) and mutant (right panel) mice; hind paws painted blue and fore paws painted red. The conditional mutant drags its hindlimb (right). (J) Rotarod analyses of control and Nestin-Cre conditional αv mutants as described in the Materials and methods. The times animals remained on the rod rotating at an increasing speed versus the trial number is plotted. A significant reduction ($P<0.005$ for all trials) in time spent on the rod is observed in mutant (n=7) versus control mice (n=9).

flox and one αv-null allele. Littermate controls were hemizygous for the hGFAP-Cre transgene, and carry one αv-flox and one αv-wild type allele.

hGFAP-Cre⁺; αv^flox/– mutants were born in expected Mendelian ratios (18 mutants from 68 total F1 progeny, or 26%). Analysis of hGFAP-Cre conditional αv mutant brains revealed that intracerebral hemorrhage occurred with 100% penetrance. P5 mutant neonates (Fig. 3K) or E18 embryos (data not shown) developed obvious punctate regions of microhemorrhage in the cerebral cortex, mid-brain and occasionally in the cerebellum (Fig. 3M; data not shown). Brains from older neonates between P7 and P14 revealed progressive reduction in cerebral microhemorrhage (data not shown), and gross and microscopic analyses of adult mutant brains revealed no obvious signs of hemorrhage or edema (Fig. 3O,Q). Immunolabeling with anti-laminin antibody revealed intact intracerebral blood vessels with no indications of distension or rupture (data not shown). Furthermore, perfusion of a small molecular weight reactive biotin tracer, revealed no obvious blood-brain barrier abnormalities in adult hGFAP-Cre conditional αv mutants (see Fig. S2 in the supplementary material).

Deletion of αv integrin in both neurons and glia also leads to cerebral vascular defects

We hypothesized that the significantly less severe hemorrhage observed in the hGFAP-Cre conditional αv mutants (as

compared with complete αv-nulls) was connected to the late onset (~E15) of Cre expression. To ablate αv expression earlier during CNS development we used a Nestin-Cre transgenic mouse strain which expresses Cre under control of a Nestin promoter (Graus-Porta et al., 2001; Haigh et al., 2003; Tronche et al., 1999). The Nestin-Cre transgene drives Cre expression primarily in CNS neural precursor cells that give rise to both neurons and glia (Haigh et al., 2003).

Nestin-Cre+; αv^+/– mice were mated with mice containing a conditional (floxed) αv allele. The resulting mutant progeny were hemizygous for the Nestin-Cre transgene, and carried one αv-flox and one αv-null allele. Littermate controls were hemizygous for the Nestin-Cre transgene, and carried one αv-flox allele and one αv wild-type allele. Cre-mediated recombination of the αv-flox allele was confirmed by PCR analysis of DNA from adult mutant brains. DNA isolated from the tail yielded PCR products of 350 and 250 bp, indicating no detectable Cre-mediated recombination (Fig. 4A,B). DNA isolated from adult brain tissue, however, showed a dramatic reduction in the 350 bp product (αv-flox), owing to Cre-mediated recombination of the αv-flox allele. The low level of 350 bp band (Fig. 4B) is probably due to the absence of Cre-mediated recombination in non-neural cells, e.g. circulating blood cells, fibroblasts, etc. Additionally, immunoblotting lysates prepared from adult cerebral cortex and cerebellum with anti-αv antibody revealed marked reduction in αv protein in Nestin-Cre conditional αv mutants (Fig. 4C). The protein
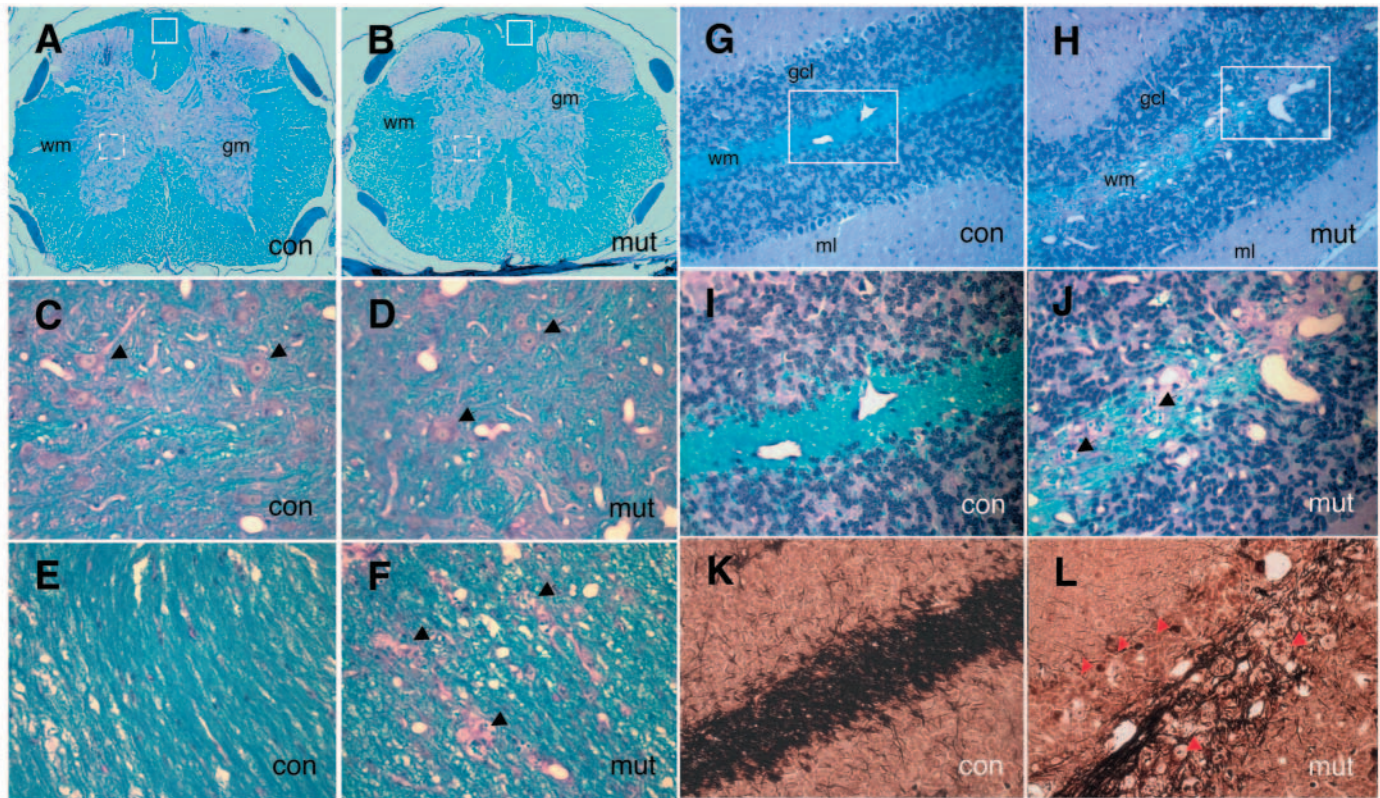
Fig. 6. Adult Nestin-Cre conditional αv mutants develop axonal degeneration in the spinal cord and cerebellum. (A,B) Cross-sections through the thoracic region of spinal cords from six-month-old control (A) and mutant (B) mice stained to visualize myelin. The axonal tracts of the white matter (wm) stain intensely blue when compared with the grey matter (gm). (C,D) Higher magnification images of grey matter (dashed boxes in A,B) from control (C) or mutant (D) spinal cords. Motoneurons in both controls and mutants are myelinated and show normal cytoarchitecture (arrows in C,D). (E,F) Higher magnification of fasciculus gracilis white matter region in control (E) and mutant (F) spinal cords (solid boxes in A,B). The myelin pattern is disorganized in the mutant, with obvious regions of macrophage infiltration (arrows in F). (G,H) Caudal cerebellar regions from 6-month-old control (G) and mutant (H) mice were stained to visualize myelin. Representative cerebellar folia are shown, with the cerebellar white matter (wm) surrounded by the granule cell layers (gcl) and molecular layers (ml). Overall cerebellum size and patterning in the control (G) and mutant (H) appear normal. (I,J) Higher magnification images from boxed regions in G,H, respectively. The mutant white matter is pale and has an abnormal pattern of myelination (H,J) when compared with the control (G,I). Macrophage infiltration is also obvious in the mutant white matter, with many macrophages containing Luxol Fast Blue-positive myelin fragments (arrows in J). (K,L) Cerebellar coronal sections from 6-month-old control (K) and mutant (L) mice silver-stained to visualize axonal neurofilaments. When compared with the control (K), there is significant axonal degeneration in the mutant cerebellum (L). Arrowheads in L indicate dystrophic axons. Also obvious in the mutant are macrophages containing silver-positive neurofilament fragments, which are indicative of axonopathy (arrows).

band at ~80 kDa (Fig. 4C) is nonspecific. It is not a fragment of full-length αv, as it is observed in αv-null cell and tissue lysates (data not shown).

Nestin-Cre conditional αv mutants were born in the expected Mendelian ratios (27 mutants of 111 total progeny, or 24%). All Nestin-Cre conditional αv mutants developed small bilateral cerebral hemorrhages beginning at E14.5, which became progressively more severe throughout embryogenesis (Fig. 4E). Gross inspection of mutant neonatal (P7) brains also revealed obvious cerebral hemorrhages (Fig. 4G,I). The cerebral hemorrhage in the Nestin-Cre conditional αv mutants was more widespread than that in the hGFAP-Cre conditional αv mutants; however, the hemorrhage was significantly less severe than that seen in the complete αv-nulls (Fig. 4H). Similar to the complete αv nulls (Bader et al., 1998), the vascular abnormalities in the Nestin-Cre conditional αv mutants initiated in the developing ganglionic eminences of the forebrain (Fig. 4K). Unlike the close juxtaposition between

cerebral vessels and the surrounding parenchyma in brains of Nestin-Cre control littermates (Fig. 4J), cerebral vessels in Nestin-Cre mutants were separated from the surrounding neural tissue (Fig. 4K). Mutant cerebral blood vessels were lined by endothelial cells and invested by a pericyte/vascular smooth muscle cell layer, but appeared tortuous and distended (Fig. 4M). Mutant neonatal brains contained abnormally high numbers of GFAP-positive astrocytes, indicative of reactive gliosis (Fig. 4Q). The increased numbers of astrocytes may represent a mechanism to repair the cerebral hemorrhage in the Nestin-Cre conditional αv mutants.

Central nervous system-specific deletion of αv integrin leads to behavioral abnormalities

Nestin-Cre conditional αv mutants survived beyond the neonatal period and were behaviorally normal until 2-3 weeks after birth. At this point, ~30% (13 of 39 mutants identified so far) began to display obvious signs of motor dysfunction (Fig.
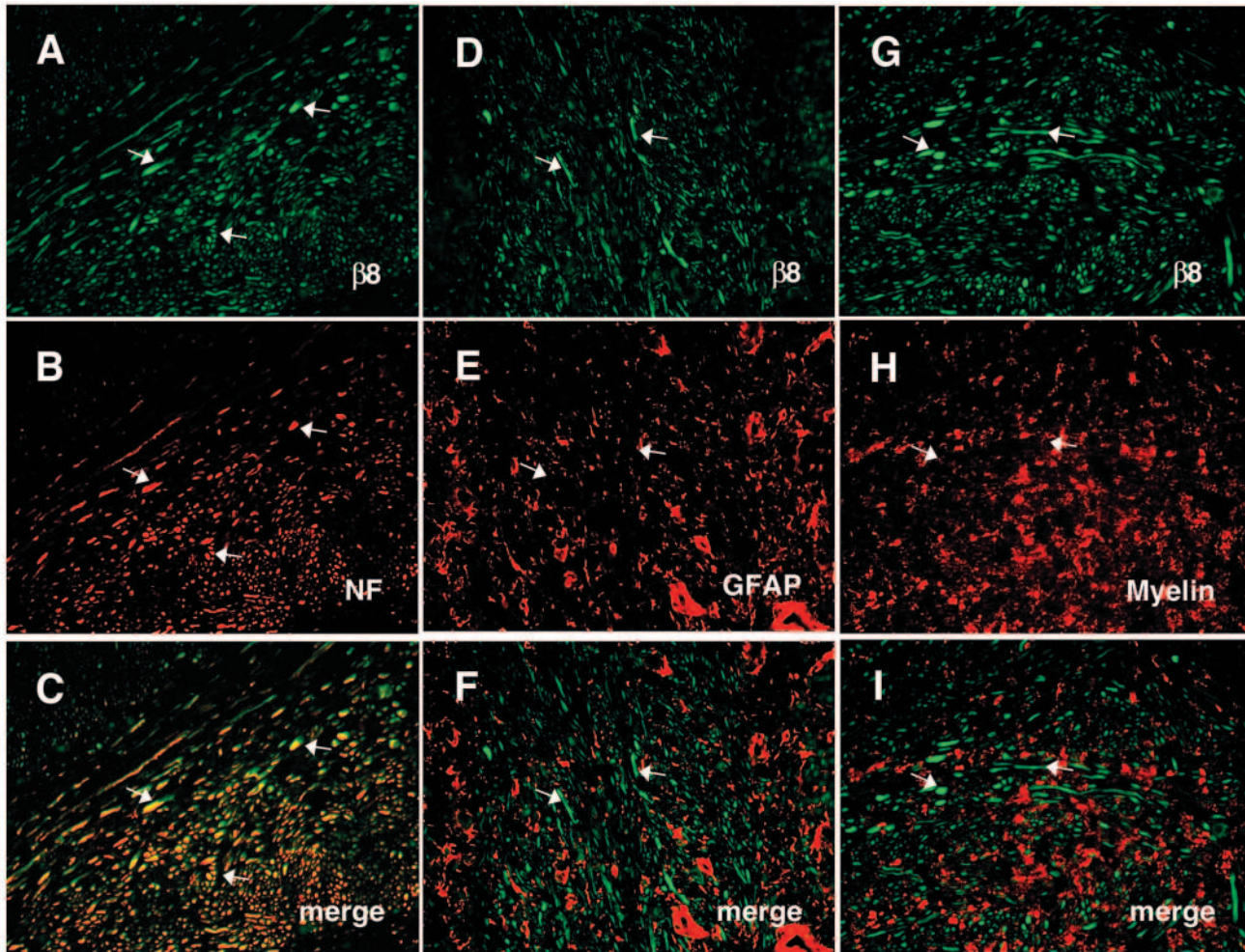
Fig. 7. αvβ8 integrin is expressed on white matter axons in the cerebellum. Coronal sections through the cerebellum of a five-month-old Nestin-Cre; αvflox/+ mouse (A-I) labeled with anti-β8 antiserum (A,D,G) and anti-neurofilament antibody to visualize axons (B), anti-GFAP antibody to visualize astrocytes (E), or anti-myelin antibody to visualize oligodendrocytes (H). (E,F,I) Merged images. αvβ8 integrin and neurofilament co-localize on white matter axons (C). In white matter regions of the cerebellum, αvβ8 is not detected on GFAP-positive astrocytes (F) or myelinating oligodendrocytes (I).

5B). These conditional αv mutants also developed spontaneous convulsions, and ultimately died by 4 weeks of age (data not shown). Histological analyses of CNS tissue isolated from mutants revealed focal regions of microhemorrhage throughout the brain and spinal cord (Fig. 5D,F). As hemorrhage begins in utero and is present prior to the onset of apparent seizure (Fig. 4E,G,I), it is very likely that the cerebral hemorrhage causes the seizures and premature death. The incomplete penetrance associated with the seizures and early death may be related to genetic heterogeneity, as the mice used in this study were a mixture of C57BL/6, 129S4 and FVB genetic backgrounds.

The remaining 70% of the Nestin-Cre mutants survived for several months. At ~2-3 months of age, 100% of these mutants began to display defects in hind limb coordination. The hind limbs of mutants remained reflexive; however, mutant muscle tone was spastic, leading to a rigid posture and gait (Fig. 5H). Indeed, gait analyses revealed that mutants partially dragged their hind limbs (Fig. 5I), and were physically weaker and less coordinated, as assessed by Rotarod testing (Fig. 5J). Mutants also displayed toe-walking, involuntary tail wriggling and

ataxia (see Movie 1 in the supplementary material; data not shown). By 6 months of age, the mutants developed more frequent seizures and more obvious symptoms of hind limb dysfunction, indicative of spastic paraparesis. Nestin-Cre mutants also developed urinary dysfunction, leading to severe bacterial infection of the bladder and, for ethical reasons, were euthanized by 8 months of age.

Nestin-Cre conditional αv mutants develop motor deficits due to axonal degeneration in the spinal cord and cerebellum

We initially expected the hindlimb dysfunction in the adult mutants to be linked to neurological damage because of persistent cerebral hemorrhage and stroke. However, gross and microscopic examination of adult mutant brains revealed no pathological indication of hemorrhage (see Fig. S3 in the supplementary material). CNS deletion of the β1 integrin subunit also leads to ataxia and premature death, largely owing to abnormal anchorage of glial end-feet to marginal zone basement membranes in the cortex and cerebellum (Graus-Porta et al., 2001). Thus, it was possible that selective loss of

αvβ1 could account for the neurological defects observed in the Nestin-Cre conditional αv mutants. However, immunofluorescence analysis of Nestin-Cre conditional αv mutants revealed normal glial end-feet attachments in the cortex and cerebellum (see Fig. S3 in the supplementary material). Histological analysis of brains from neonatal and adult Nestin-Cre mutants, both by Hematoxylin and Eosin staining, as well as immunohistochemistry using an antibody directed against the neuronal nuclear marker NeuN, revealed relatively normal neuronal patterning in the cerebral cortex and cerebellum (see Fig. S3 in the supplementary material; data not shown). Additionally, silver staining to label axonal neurofilaments, or immunohistochemistry using an anti-MAP2 antibody to label dendrites, revealed normal neuronal arborizations (see Fig. S3 in the supplementary material; data not shown).

We also suspected that the onset of spastic paraparesis in the Nestin-Cre conditional αv mutants might be due to neuromuscular defects. However, examination of mutant quadriceps showed no indications of muscular atrophy or wasting (see Fig. S4 in the supplementary material). Furthermore, inspection of hindlimb peripheral nerves as well as peripheral nerves connecting to thoracic and lumbar spinal cord dorsal root ganglia revealed no obvious pathological indication of peripheral axonal degeneration or demyelination (see Fig. S4 in the supplementary material; data not shown). This is unlike the paralysis and demyelination defects observed in mutant mice where β1 integrin is selectively ablated in peripheral nervous system Schwann cells (Feltri et al., 2002).

Analyses of grey matter spinal cord regions from controls and Nestin-Cre conditional αv mutants did not reveal motor neuron dystrophy or degeneration (Fig. 6C,D). However, analysis of spinal cord white matter revealed demyelination (Fig. 6F) and axonal dystrophy (data not shown) within the fasciculus gracilis, an axonal tract that regulates hind limb proprioception and discriminative touch. Additionally, an obvious macrophage infiltrate was present, with many macrophages containing myelin fragments (Fig. 6F) as well as axonal fragments (data not shown), suggesting both glial and axonal degeneration.

Axons of the cerebellar white matter also regulate basic hind limb proprioception and coordination (Bosco and Poppele, 2003). Luxol Fast Blue staining to visualize myelin revealed significant demyelination in the caudal cerebellum of Nestin-Cre conditional αv mutants (Fig. 6J). Additionally, analysis of silver-stained white matter axons within the cerebellum revealed obvious axonopathy (Fig. 6L). A macrophage infiltrate was also present, and many macrophages contained internalized myelin and neurofilament fragments (Fig. 6J,L). However, a lymphocyte infiltrate, which would be indicative of autoimmunity, was not present in the spinal cord or cerebellar lesions.

αvβ8 integrin is expressed on axons in the cerebellum

Ablation of the β8 gene leads to a cerebral hemorrhage phenotype (Zhu et al., 2002), which is essentially identical to that observed in the complete αv-nulls (Bader et al., 1998). With this knowledge, we hypothesized that the neurological defects observed in the Nestin-Cre conditional αv mutants were probably due to the selective loss of αvβ8 function. To determine the expression pattern for αvβ8 protein in the adult cerebellum, we used an antibody directed against the β8 integrin subunit (Fig. 7A,D,G). αvβ8 was expressed on axons in the caudal cerebellum, as determined by co-localization with an anti-neurofilament antibody (Fig. 7C). However, αvβ8 was not detected on cerebellar white matter astrocytes (Fig. 7F) or oligodendrocytes (Fig. 7I). αvβ8 protein was also expressed on spinal cord axons, including the fasciculus gracilis (data not shown). Interestingly, αvβ8 was also expressed on axons in white matter regions of the cerebral cortex (data not shown), although no pathological lesions were observed in these regions at the time of death.

Discussion

We have used Cre/Lox technology to analyze the functions of αv integrins in the embryonic and postnatal CNS. Selective ablation of αv expression in endothelial cells does not produce any obvious embryonic or neonatal developmental defects. By contrast, ablation of αv expression on neural cells, particularly glia, has significant effects. A central result from this work is that αvβ8 integrin expressed on embryonic CNS neural cells is necessary for the proper development of cerebral blood vessels. This finding extends our earlier studies of complete αv-null mice (McCarty et al., 2002), and firmly implicates αvβ8 as a neural regulator of embryonic cerebral blood vessel function. Additionally, we present the novel finding that αvβ8 integrin expressed on CNS axons plays an important function in mediating long-term axonal survival. Collectively, these results suggest that αvβ8 may function in mediating proper cellular juxtaposition both between neural cells and blood vessels in the embryonic CNS, and between axons and glia in the postnatal CNS.

αvβ8 integrin on embryonic CNS neural cells is necessary for proper cerebral blood vessel development

Cerebral blood vessels are composed of endothelial cells and pericytes surrounded by a vascular basement membrane. The close juxtaposition between cerebral blood vessels and surrounding neural cells, particularly glia, evokes an attractive model, whereby αvβ8 integrin on the glial processes mediates interactions with blood vessels via adhesion to ECM ligands within the vascular basement membrane. Neural cell adhesion via αvβ8 may provide physical support that maintains proper blood vessel morphology. Alternatively, αvβ8 may play a more dynamic role in mediating the adhesion and communication between neural cells and blood vessels. We propose a model where αvβ8 integrin is necessary for the initiation and maintenance of neural cell-blood vessel adhesion and communication, perhaps including proper assembly of the basement membrane. A wave of secondary events would then serve to affect proper neural cell-blood vessel juxtaposition. We are currently identifying and characterizing the signal transduction pathways activated by αvβ8 adhesion in an attempt to understand better neural cell-mediated regulation of cerebral blood vessel development.

Differences between conditional αv-null and complete αv-null phenotypes

Why do 100% of complete αv-nulls die by the first day of birth,

whereas the majority of the conditional αv mutants survive for several months? First, conditional αv mutants do not develop other non-CNS abnormalities that occur with variable penetrance in complete αv-nulls (Bader et al., 1998). Second, the hemorrhage in the conditional αv knockout mice is significantly less severe than that in the complete αv-nulls, most probably because of differences in Cre spatial expression. Additionally, there may be a temporal delay from the onset of Cre expression (and αv-flox deletion) to the point where αv integrin mRNA and protein are completely absent from the cells. Last, epigenetic events may preclude all glial cells from efficiently recombining the αv-flox allele, leading to a mosaic pattern of Cre expression. Such mosaic Cre expression would decrease the overall proportion of αv-null glial cells, thus leading to a reduction in the severity of hemorrhage. Alternatively, it is possible that loss of αv expression on multiple CNS cell types is necessary to recapitulate fully the severe cerebral hemorrhage observed in the complete αv-nulls.

αvβ8 integrin mediates long-term axonal survival

We initially hypothesized that the neurological phenotypes observed in the adult Nestin-Cre conditional αv mutants were the result of CNS trauma caused by the early embryonic and neonatal hemorrhage. Indeed, this is the case for humans with various forms of cerebral palsy, where localized CNS trauma during prenatal or neonatal periods leads to neuronal cell death and the unfortunate symptoms associated with this disease (Ozduman et al., 2004). However, the hemorrhage in the Nestin-Cre conditional αv mutants occurs throughout the embryonic and neonatal brain, whereas the neurological lesions first develop in specific regions of the adult spinal cord and cerebellum, suggesting a more localized defect responsible for the neurological phenotype.

Alternatively, the neurological lesions may result from progressive hydrocephaly resulting from intraventricular hemorrhage. Indeed, complete αv-null mutants develop intraventricular hemorrhage as early as E12.5, and display severe hydrocephaly at birth (Bader et al., 1998). Interestingly, severe hydrocephaly in humans can cause pathological lesions in the long white matter tracts of the cerebral cortex and cerebellum, leading to symptoms such as seizures, ataxia, lower limb spasticity and urinary dysfunction (Silverberg, 2004). However, we have yet to observe intraventricular hemorrhage or obvious hydrocephalus in the Nestin-Cre conditional αv mutants. Nonetheless, it remains possible that subtle changes in ventricle volume may account for some of the neurological abnormalities.

A more likely explanation for the neurological phenotypes, and one supported by our experimental data, is that the adult-onset defects are unrelated to the embryonic and neonatal hemorrhage. Indeed, to date, no neurological defects or premature death are observed in the hGFAP-Cre conditional αv mutants, which also develop embryonic and neonatal cerebral hemorrhage, albeit less severe than we see in the Nestin-Cre conditional αv mutants. Additionally, the progressive neurological phenotypes observed in the Nestin-Cre conditional αv mutants develop over a period of several months, well beyond the time of embryonic and neonatal hemorrhage. Last, αvβ8 integrin protein is expressed on axons in the spinal cord and cerebellum where pathologic lesions develop in the Nestin-Cre conditional αv mutants. These data

collectively suggest that the CNS abnormalities observed in the Nestin-Cre conditional αv mutants are likely to be related to the specific loss of αvβ8, as they do not occur in β3/β5 integrin double knockout mice (McCarty et al., 2002), or β6 integrin knockouts (Huang et al., 1996), and are distinct from the neurological defects in mice lacking β1 integrins in the CNS or PNS (Graus-Porta et al., 2001; Feltri et al., 2002). The confirmation of this hypothesis awaits generation and analysis of conditional β8 knockout mice.

Interestingly, in the Nestin-Cre conditional αv mutants, we observe not only spinocerebellar axonal degeneration, but also significant demyelination. Thus, analogous to its role in regulating glia-blood vessel juxtaposition, axonally expressed αvβ8 may also mediate proper axonal-glial interactions. CNS axons intimately associate with myelinating oligodendrocytes via direct cell-cell contacts, as well as cell-ECM adhesion. Recent evidence also shows cooperative signaling between integrins and a variety of axonal guidance and survival factors, including the Ephs/ephrins (Zou et al., 1999), semaphorins (Pasterkamp et al., 2003), netrins (Yebra et al., 2003) and slits (Stevens and Jacobs, 2002). It will be interesting to determine whether αvβ8 integrin signaling events 'crosstalk' with these other pathways, and how these events may regulate axonal survival.

αv mutants and human genetic diseases

The cerebral hemorrhage in the conditional αv mutants is very similar to pathologies associated with the human genetic disorder cerebral cavernous malformation (CCM). Individuals with CCM develop CNS hemorrhage characterized by tortuous blood vessels devoid of surrounding brain parenchyma, leading to clinical symptoms ranging from mild headaches to sporadic seizures and loss of motor function (Marchuk et al., 2003). Mutations in the *KRIT1* gene have been linked to ~50% of all familial CCM cases (Gunel et al., 2002; Laberge-le Couteulx et al., 1999). We are currently investigating whether αvβ8 integrin plays a role in regulating Krit1 function and how these events may be connected to development of CCM.

Finally, the neurological abnormalities observed in the adult Nestin-Cre conditional αv mutants are similar to a human genetic disorder known as hereditary spastic paraparesis (HSP) (Kobayashi et al., 1996; McDermott et al., 2000). Individuals with HSP develop progressive lower limb spasticity partly because of deterioration of spinocerebellar axons. It will be interesting to determine if the Nestin-Cre conditional αv mutants might serve as a useful mouse model for studying the pathogenesis and treatment of symptoms related to HSP.

Supplementary material

Supplementary material for this article is available at
http://dev.biologists.org/cgi/content/full/132/1/165/DC1

References

Allende, M. L., Yamashita, T. and Proia, R. L. (2003). G-protein-coupled receptor S1P1 acts within endothelial cells to regulate vascular maturation. *Blood* **102**, 3665-3667.

Anthony, T. E., Klein, C., Fishell, G. and Heintz, N. (2004). Radial glia serve as neuronal progenitors in all regions of the central nervous system. *Neuron* **41**, 881-890.

Anton, E. S., Kreidberg, J. A. and Rakic, P. (1999). Distinct functions of alpha3 and alpha(v) integrin receptors in neuronal migration and laminar organization of the cerebral cortex. *Neuron* **22**, 277-289.

Bader, B. L., Rayburn, H., Crowley, D. and Hynes, R. O. (1998). Extensive vasculogenesis, angiogenesis, and organogenesis precede lethality in mice lacking all αv integrins. *Cell* **95**, 507-519.

Bajenaru, M. L., Zhu, Y., Hedrick, N. M., Donahoe, J., Parada, L. F. and Gutmann, D. H. (2002). Astrocyte-specific inactivation of the neurofibromatosis 1 gene (NF1) is insufficient for astrocytoma formation. *Mol. Cell Biol.* **22**, 5100-5113.

Bosco, G. and Poppele, R. (2003). Cerebellar afferent systems: can they help us understand cerebellar function? *Cerebellum* **2**, 162-164.

Bossy, B. and Reichardt, L. F. (1990). Chick integrin alpha V subunit molecular analysis reveals high conservation of structural domains and association with multiple beta subunits in embryo fibroblasts. *Biochemistry* **29**, 10191-10198.

Feltri, M. L., Graus Porta, D., Previtali, S. C., Nodari, A., Migliavacca, B., Cassetti, A., Littlewood-Evans, A., Reichardt, L. F., Messing, A., Quattrini, A. et al. (2002). Conditional disruption of beta 1 integrin in Schwann cells impedes interactions with axons. *J. Cell Biol.* **156**, 199-209.

Gerety, S. S. and Anderson, D. J. (2002). Cardiovascular ephrinB2 function is essential for embryonic angiogenesis. *Development* **129**, 1397-1410.

Graus-Porta, D., Blaess, S., Senften, M., Littlewood-Evans, A., Damsky, C., Huang, Z., Orban, P., Klein, R., Schittny, J. C. and Muller, U. (2001). Beta1-class integrins regulate the development of laminae and folia in the cerebral and cerebellar cortex. *Neuron* **31**, 367-379.

Gunel, M., Laurans, M. S., Shin, D., DiLuna, M. L., Voorhees, J., Choate, K., Nelson-Williams, C. and Lifton, R. P. (2002). KRIT1, a gene mutated in cerebral cavernous malformation, encodes a microtubule-associated protein. *Proc. Natl. Acad. Sci. USA* **99**, 10677-10682.

Haigh, J. J., Morelli, P. I., Gerhardt, H., Haigh, K., Tsien, J., Damert, A., Miquerol, L., Muhlner, U., Klein, R., Ferrara, N. et al. (2003). Cortical and retinal defects caused by dosage-dependent reductions in VEGF-A paracrine signaling. *Dev. Biol.* **262**, 225-241.

Harlowe, E. and Lane, D. (1999). In *Using Antibodies: A Laboratory Approach*, p. 437. Cold Spring Harbor, NY: Cold Spring Harbor Laboratory Press.

Hirsch, E. G. D., Balzac, F., Altruda, F., Silengo, L. and Tarone, G. (1994). Alpha v integrin subunit is predominantly located in nervous tissue and skeletal muscle during mouse development. *Dev. Dyn.* **201**, 108-120.

Huang, X. Z., Wu, J. F., Cass, D., Erle, D. J., Corry, D., Young, S. G., Farese, R. V., Jr and Sheppard, D. (1996). Inactivation of the integrin beta 6 subunit gene reveals a role of epithelial integrins in regulating inflammation in the lung and skin. *J. Cell Biol.* **133**, 921-928.

Kisanuki, Y. Y., Hammer, R. E., Miyazaki, J., Williams, S. C., Richardson, J. A. and Yanagisawa, M. (2001). Tie2-Cre transgenic mice: a new model for endothelial cell-lineage analysis in vivo. *Dev. Biol.* **230**, 230-242.

Kobayashi, H., Garcia, C. A., Alfonso, G., Marks, H. G. and Hoffman, E. P. (1996). Molecular genetics of familial spastic paraplegia: a multitude of responsible genes. *J. Neurol. Sci.* **137**, 131-138.

Laberge-le Couteulx, S., Jung, H. H., Labauge, P., Houtteville, J. P., Lescoat, C., Cecillon, M., Marechal, E., Joutel, A., Bach, J. F. and Tournier-Lasserve, E. (1999). Truncating mutations in CCM1, encoding KRIT1, cause hereditary cavernous angiomas. *Nat. Genet.* **23**, 189-193.

Liao, Y., Day, K. H., Damon, D. N. and Duling, B. R. (2001). Endothelial cell-specific knockout of connexin 43 causes hypotension and bradycardia in mice. *Proc. Natl. Acad. Sci. USA* **98**, 9989-9994.

Louissaint, A., Jr, Rao, S., Leventhal, C. and Goldman, S. A. (2002). Coordinated interaction of neurogenesis and angiogenesis in the adult songbird brain. *Neuron* **34**, 945-960.

Malatesta, P., Hack, M. A., Hartfuss, E., Kettenmann, H., Klinkert, W., Kirchhoff, F. and Gotz, M. (2003). Neuronal or glial progeny: regional differences in radial glia fate. *Neuron* **37**, 751-764.

Marchuk, D. A., Srinivasan, S., Squire, T. L. and Zawistowski, J. S. (2003). Vascular morphogenesis: tales of two syndromes. *Hum. Mol. Genet.* **12**, R97-R112.

Marino, S., Vooijs, M., van Der Gulden, H., Jonkers, J. and Berns, A.

(2000). Induction of medulloblastomas in p53-null mutant mice by somatic inactivation of Rb in the external granular layer cells of the cerebellum. *Genes Dev.* **14**, 994-1004.

McCarty, J. H., Monahan-Earley, R. A., Brown, L. F., Keller, M., Gerhardt, H., Rubin, K., Shani, M., Dvorak, H. F., Wolburg, H., Bader, B. L. et al. (2002). Defective associations between blood vessels and brain parenchyma lead to cerebral hemorrhage in mice lacking alphav integrins. *Mol. Cell. Biol.* **22**, 7667-7677.

McDermott, C., White, K., Bushby, K. and Shaw, P. (2000). Hereditary spastic paraparesis: a review of new developments. *J. Neurol. Neurosurg. Psych.* **69**, 150-160.

Mi, H., Haeberle, H. and Barres, B. A. (2001). Induction of astrocyte differentiation by endothelial cells. *J. Neurosci.* **21**, 1538-1547.

Milner, R., Huang, X., Wu, J., Nishimura, S., Pytela, R., Sheppard, D. and ffrench-Constant, C. (1999). Distinct roles for astrocyte αvβ5 and αvβ8 integrins in adhesion and migration. *J. Cell Sci.* **112**, 4271-4279.

Mu, D., Cambier, S., Fjellbirkeland, L., Baron, J. L., Munger, J. S., Kawakatsu, H., Sheppard, D., Broaddus, V. C. and Nishimura, S. L. (2002). The integrin alpha(v)beta8 mediates epithelial homeostasis through MT1-MMP-dependent activation of TGF-beta1. *J. Cell Biol.* **157**, 493-507.

Nishimura, S., Sheppard, D. and Pytela, R. (1994). Integrin αvβ8: interaction with vitronectin and functional divergence of the β8 cytoplasmic domain. *J. Biol. Chem.* **269**, 28708-28715.

Nishimura, S., Boylen, K., Einheber, S., Milner, T., Ramos, D., Pytela, R. (1998). Synaptic and glial localization of the integrin αvβ8 in mouse and rat brain. *Brain Res.* **791**, 271-282.

Ozduman, K., Pober, B. R., Barnes, P., Copel, J. A., Ogle, E. A., Duncan, C. C. and Ment, L. R. (2004). Fetal stroke. *Pediatr. Neurol.* **30**, 151-162.

Palmer, T. D., Willhoite, A. R. and Gage, F. H. (2000). Vascular niche for adult hippocampal neurogenesis. *J. Comp. Neurol.* **425**, 479-494.

Pasterkamp, R. J., Peschon, J. J., Spriggs, M. K. and Kolodkin, A. L. (2003). Semaphorin 7A promotes axon outgrowth through integrins and MAPKs. *Nature* **424**, 398-405.

Silverberg, G. D. (2004). Normal pressure hydrocephalus (NPH): ischaemia, CSF stagnation or both. *Brain* **127**, 947-948.

Song, H., Stevens, C. F. and Gage, F. H. (2002). Astroglia induce neurogenesis from adult neural stem cells. *Nature* **417**, 39-44.

Soriano, P. (1999). Generalized lacZ expression with the ROSA26 Cre reporter strain. *Nat. Genet.* **21**, 70-71.

Stevens, A. and Jacobs, J. R. (2002). Integrins regulate responsiveness to slit repellent signals. *J. Neurosci.* **22**, 4448-4455.

Tronche, F., Kellendonk, C., Kretz, O., Gass, P., Anlag, K., Orban, P. C., Bock, R., Klein, R. and Schutz, G. (1999). Disruption of the glucocorticoid receptor gene in the nervous system results in reduced anxiety. *Nat. Genet.* **23**, 99-103.

Venstrom, K. and Reichardt, L. (1995). β8 integrins mediate interactions of chick sensory neurons with laminin-1, collagen IV, and fibronectin. *Mol. Biol. Cell* **6**, 419-431.

Yebra, M., Montgomery, A. M., Diaferia, G. R., Kaido, T., Silletti, S., Perez, B., Just, M. L., Hildbrand, S., Hurford, R., Florkiewicz, E. et al. (2003). Recognition of the neural chemoattractant Netrin-1 by integrins alpha6beta4 and alpha3beta1 regulates epithelial cell adhesion and migration. *Dev. Cell* **5**, 695-707.

Zerlin, M. and Goldman, J. E. (1997). Interactions between glial progenitors and blood vessels during early postnatal corticogenesis: blood vessel contact represents an early stage of astrocyte differentiation. *J. Comp. Neurol.* **387**, 537-546.

Zhu, J., Motejlek, K., Wang, D., Zang, K., Schmidt, A. and Reichardt, L. F. (2002). beta8 integrins are required for vascular morphogenesis in mouse embryos. *Development* **129**, 2891-2903.

Zhuo, L., Theis, M., Alvarez-Maya, I., Brenner, M., Willecke, K. and Messing, A. (2001). hGFAP-cre transgenic mice for manipulation of glial and neuronal function in vivo. *Genesis* **31**, 85-94.

Zou, J. X., Wang, B., Kalo, M. S., Zisch, A. H., Pasquale, E. B. and Ruoslahti, E. (1999). An Eph receptor regulates integrin activity through R-Ras. *Proc. Natl. Acad. Sci. USA* **96**, 13813-13818.